

Density of state and non-magnetic impurity effects in electron-doped cuprates

Bin Liu¹ and Ying Liang²

¹ *Max-Planck-Institut für Physik komplexer Systeme, D-01187 Dresden, Germany*

² *Department of Physics, Beijing Normal University, Beijing 100875, China*

we analyze the density of state (DOS) and a non-magnetic impurity effect in electron-doped cuprates starting from two different scenarios: the $d_{x^2-y^2}$ -wave superconductivity coexisting with antiferromagnetic spin density wave (SDW) order versus $d_{x^2-y^2}$ -wave superconductivity with a higher harmonic. We find that in both cases the local density of state (LDOS) exhibits two impurity-induced resonance states at low energies. We also find that for the intermediate value of the SDW gap, the DOS looks similar to that obtained from the scenario of the $d_{x^2-y^2}$ -wave gap with a higher harmonic, suggesting the presence of a non-monotonic $d_{x^2-y^2}$ -wave gap. However, if the SDW gap is sufficiently large the DOS looks more conventional s-wave like. This obvious difference from the DOS resulted from the $d_{x^2-y^2}$ -wave gap with a higher harmonic model, could differentiate the two above scenarios and is needed to be proved in the further doping dependence of tunneling spectrum measurement.

PACS numbers: 74.72.Jt, 74.20.Mn, 74.25.Ha, 74.25.Jb

I. INTRODUCTION

The electron-doped cuprate high-temperature superconductors have recently attracted a considerable attention due to their considerable asymmetry from hole-doped ones. For instance, it has been known that in contrast to the hole-doped cuprates, the electron-doped systems show (i) relatively low superconducting transition temperature, (ii) narrow superconducting (SC) region in the phase diagram, and (iii) the robust antiferromagnetic (AF) order¹.

The phase sensitive scanning SQUID measurements², nuclear magnetic resonance study³, and also ARPES experiments^{4,5} have provided strong evidences that the electron-doped superconductors are the $d_{x^2-y^2}$ -wave superconductors. This conclusion seems to be natural, since from the theoretical point of view, the same pairing mechanism is expected both for hole- and electron-doped materials, although the functional form of the $d_{x^2-y^2}$ -wave gap in electron-doped materials is more subtle issue. The high-resolution ARPES data on the leading-edge gap in $Pr_{0.89}LaCe_{0.11}CuO_4$ ⁴, Raman experiments in $NCCO$ ⁶, and doping dependence of tunneling study in $Pr_{2-x}Ce_xCuO_{4-\delta}$ ⁷ show a non-monotonic $d_{x^2-y^2}$ -wave gap with a maximum value in between nodal and antinodal points on the Fermi surface (FS), and meanwhile the measurements of optical conductivity $\sigma_1(\omega)$ in $Pr_{1.85}Ce_{0.15}CuO_4$ ⁸ were also interpreted as an indirect evidence of a non-monotonic $d_{x^2-y^2}$ -wave gap.

The theoretical explanations for the origin of the non-monotonic gap behavior are classified into two scenarios so far. One is the coexisting AF with SC order scenario^{9,10}. Although the SC gap itself is assumed to be monotonic $d_{x^2-y^2}$ -wave, when the AF order is introduced, the resulting quasiparticle excitation can be gapped by both orders and behaves to be non-monotonic $d_{x^2-y^2}$ -wave gap. The other one is to extend the SC gap out of the simplest $d_{x^2-y^2}$ -wave via the inclusion of a higher harmonic term^{11,12}. From theory perspective,

the non-monotonic $d_{x^2-y^2}$ -wave gap appears naturally under the assumption that the $d_{x^2-y^2}$ -wave pairing is caused by the interaction with the continuum of overdamped AF spin fluctuations. Spin-mediated interaction is attractive in the $d_{x^2-y^2}$ -wave channel and yields a gap which is maximal near the hot spots - the points along the FS, separated by AF moment Q_{AF} . In optimally doped $NCCO$ and $PCCO$, hot spots are located close to Brillouin zone diagonals, and one should generally expect the $d_{x^2-y^2}$ -wave gap to be non-monotonic. In this case, the non-monotonic gap behavior is an intrinsic property in the SC state regardless of the presence of the AF order.

In fact, impurity effect has always been used as one of the most important and effective tools to distinguish pairing symmetry in the conventional and unconventional superconductors. It has been known that the Yu-Shiba-Rusinov state in the conventional BCS superconductor (s-wave) was located at the gap edge¹³. However in the $d_{x^2-y^2}$ -wave superconductor an impurity-induced bound state appear near the Fermi energy¹⁴. The origin of this difference has been explained as different phase structure of two kinds of SC order: $d_{x^2-y^2}$ -wave pairing symmetry with the line nodal gap while s-wave symmetry with nodeless gap. Therefore, we in this paper analyze the DOS and a non-magnetic impurity effect starting from two different scenarios: the $d_{x^2-y^2}$ -wave superconductivity coexisting with AF SDW wave order versus $d_{x^2-y^2}$ -wave superconductivity with a higher harmonic. We find that in both cases the LDOS exhibits two impurity-induced resonance states at low energies. We also find that for the intermediate value of the SDW gap, the DOS looks similar to that obtained from the scenario of the $d_{x^2-y^2}$ -wave gap with a higher harmonic, suggesting the presence of a non-monotonic $d_{x^2-y^2}$ -wave gap. However, if the SDW gap is sufficiently large the DOS looks more conventional s-wave like instead of the non-monotonic $d_{x^2-y^2}$ -wave gap behavior. This obvious difference from the DOS resulted from the $d_{x^2-y^2}$ -wave gap with a higher harmonic model even in the underdoped

regimes, could differentiate the two above scenarios. Our results strongly suggest the further doping dependence of tunneling spectrum measurement, especially in the underdoped regimes, is needed to be carried out so as to shed light on the physical origin of the unusual non-monotonic gap in the electron-doped cuprates.

II. THE MODEL AND T-MATRIX FORMULATION

We start from a phenomenological superconducting Hamiltonian on a square lattice at the mean field level,

$$\begin{aligned} H &= H_{SC} + H_{SDW}, \\ H_{SC} &= \sum_{\mathbf{k}\sigma} [(\varepsilon_{\mathbf{k}} - \mu)c_{\mathbf{k}\sigma}^\dagger c_{\mathbf{k}\sigma} \\ &\quad + \Delta_{\mathbf{k}}(c_{\mathbf{k}\uparrow}^\dagger c_{-\mathbf{k}\downarrow}^\dagger + c_{-\mathbf{k}\downarrow} c_{\mathbf{k}\uparrow})], \\ H_{SDW} &= - \sum_{\mathbf{k}\sigma} M\sigma(c_{\mathbf{k}\sigma}^\dagger c_{\mathbf{k}+\mathbf{Q}\sigma} + h.c.), \end{aligned} \quad (1)$$

where $c_{\mathbf{k}\sigma}^\dagger$ ($c_{\mathbf{k}\sigma}$) is the fermion creation (destruction) operator and μ is chemical potential. The SC order parameter has the usual form $\Delta_{\mathbf{k}} = \Delta(\cos(k_x) - \cos(k_y))/2$ and the AF SDW order parameter is M . We take the normal state tight binding dispersion $\varepsilon_{\mathbf{k}}$, which is written as

$$\begin{aligned} \varepsilon_{\mathbf{k}} &= -2t(\cos(k_x) + \cos(k_y)) - 4t_1 \cos(k_x) \cos(k_y) \\ &\quad - 2t_2(\cos(2k_x) + \cos(2k_y)) \\ &\quad - 4t_3(\cos(2k_x) \cos(k_y) + \cos(k_x) \cos(2k_y)) \\ &\quad - 4t_4 \cos(2k_x) \cos(2k_y) \end{aligned} \quad (2)$$

with $t = 120$ meV, $t_1 = -60$ meV, $t_2 = 34$ meV, $t_3 = 7$ meV, $t_4 = 20$ meV, and $\mu = -82$ meV at 0.11 doping¹⁵ reproducing the underlying FS as inferred from recent ARPES experiment⁴. Note that here the wave vector \mathbf{k} is restricted to the magnetic Brillouin zone (MBZ).

It is convenient to introduce a 4×4 matrix formulation to treat the coexisting SDW and SC phase. After taking a four-component Nambu spinor $\Psi_{\mathbf{k}} = (c_{\mathbf{k}\uparrow}, c_{\mathbf{k}+\mathbf{Q}\uparrow}, c_{-\mathbf{k}\downarrow}^\dagger, c_{-\mathbf{k}-\mathbf{Q}\downarrow}^\dagger)^\top$ with $\mathbf{Q} = (\pi, \pi)$ being the nesting vector, we rewrite the Hamiltonian as

$$H = \sum_{\mathbf{k}} \Psi_{\mathbf{k}}^\dagger ((\varepsilon_{\mathbf{k}} - \mu)\tau_3\rho_0 + M\tau_1\rho_0 + \Delta_{\mathbf{k}}\tau_3\rho_1)\Psi_{\mathbf{k}}, \quad (3)$$

where $\tau_3\rho_1 = \begin{pmatrix} 0 & \tau_3 \\ \tau_3 & 0 \end{pmatrix}$. Then the single-particle matrix Green's function is determined as $G_0^{-1}(k, i\omega_n) = i\omega_n - (\varepsilon_{\mathbf{k}} - \mu)\tau_3\rho_0 - M\tau_1\rho_0 - \Delta_{\mathbf{k}}\tau_3\rho_1$.

The scattering of quasiparticles from the impurity is described by a T-matrix^{14,16,17}, $T(i\omega_n)$, which is local and independent of wave vectors. Thus, we define the 2×2 Green's function in the presence of a single impurity as

$$\begin{aligned} G(i, j; i\omega_n) &= \zeta_0(i - j; i\omega_n) \\ &\quad + \zeta_0(i, i\omega_n)T(i\omega_n)\zeta_0(j, i\omega_n), \end{aligned} \quad (4)$$

where

$$\begin{aligned} \zeta_0(i, j; i\omega_n) &= \frac{1}{N} \sum_{\mathbf{k}} e^{i\mathbf{k}\cdot\mathbf{R}_{ij}} \\ &\quad \times \begin{pmatrix} G_0^1(k, i\omega_n) & G_0^2(k, i\omega_n) \\ G_0^3(k, i\omega_n) & G_0^4(k, i\omega_n) \end{pmatrix}, \end{aligned} \quad (5)$$

with

$$\begin{aligned} G_0^{\mathbf{I}}(k, i\omega_n) &= e^{-i\mathbf{Q}\cdot\mathbf{R}_j}[G_0]_{\mathbf{I}}^{12}(k, i\omega_n) + e^{i\mathbf{Q}\cdot\mathbf{R}_i}[G_0]_{\mathbf{I}}^{21}(k, i\omega_n) \\ &\quad + e^{i\mathbf{Q}\cdot\mathbf{R}_{ij}}[G_0]_{\mathbf{I}}^{22}(k, i\omega_n) + [G_0]_{\mathbf{I}}^{11}(k, i\omega_n). \end{aligned} \quad (6)$$

Here $\mathbf{I} = 1, 2, 3, 4$ denotes the left-top, right-top, left-bottom and right-bottom 2×2 block element of $G_0(k, i\omega_n)$, and \mathbf{R}_i is lattice vector and $\mathbf{R}_{ij} = \mathbf{R}_i - \mathbf{R}_j$. The T-matrix can be written by

$$T(i\omega_n) = \frac{U_0\rho_3}{1 - U_0\rho_3\zeta_0(0, 0; i\omega_n)}. \quad (7)$$

For the d-wave pairing symmetry, one can find that the local Green's function $\zeta_0(i, i; i\omega_n)$ is diagonal. As a result, the diagonal T-matrix

$$T_{11,22}(i\omega_n) = \frac{\pm U_0}{1 - U_0[\zeta_0(0, 0; \pm i\omega_n)]_{11}} \quad (8)$$

where the upper (lower) sign denotes T_{11} (T_{22}), will give rise to a particle- ($\omega_{res} < 0$) and hole-like ($\omega_{res} > 0$) resonance state. These resonance states generate the sharp peaks in the LDOS only in the unitary limit ($|\omega_{res}|/\Delta \leq 1$) where $1 = U_0 \text{Re}[\zeta_0(0, 0; \pm\omega_{res})]_{11}$. Finally, these above equations allow a complete solution of the problem as long as the order-parameter relaxation can be neglected.

III. NUMERICAL RESULTS AND DISCUSSIONS

A. $d_{x^2-y^2}$ -wave coexisting with AF SDW order

We firstly calculate the DOS

$$\rho(\omega) = -\frac{1}{\pi} \text{Im} \sum_{ik} G_{ii}(k, \omega) \quad (9)$$

plotted in Fig.1 for different SDW gap (M). In principle, SDW gap (M) and SC gap (Δ) need to be solved self-consistently. For simplicity, we in the following calculation choose $\Delta = 0.005eV$ reproducing the ARPES estimate of SC gap in $Pr_{0.89}LaCe_{0.11}CuO_4$ ⁴, and different values of SDW gap $M = 0.14, 0.12, 0.05$, and $0(eV)$, where the maximal value $M = 0.14(eV)$ is a self-consistent value from Ref.15 at doping $x = 0.11$, and the gradually decreasing values with the independent band dispersion (Eq.(2)) corresponds to the increasing doping^{15,18,19}. In this case, our SDW gap dependence of DOS can be qualitatively equivalent to the doping evolution of DOS.

In the coexisting AF SDW and SC state, there are three features of interest. First, at low energies the DOS spectrum remains d-wave like superconductor behavior for fairly large values M . Second, with the increasing of M , besides the coherent peak located at the SC gap, another two new “coherent peaks” appear symmetrically at positive and negative low energy, and the positions of these peaks shift towards the Fermi energy, indicating the presence of non-monotonic $d_{x^2-y^2}$ -wave gap behavior. The third and last feature is that at sufficiently large SDW gap M , the DOS shows the U-shaped behavior instead of the non-monotonic $d_{x^2-y^2}$ -wave gap behavior. This U-shaped DOS has been observed in earlier point contact tunneling spectrum and was explained as the character of s-wave pairing^{6,20,21}, but in present case it is the result of the coexisting SDW and SC orders, the difference between them will be differentiated by considering a non-magnetic impurity effect.

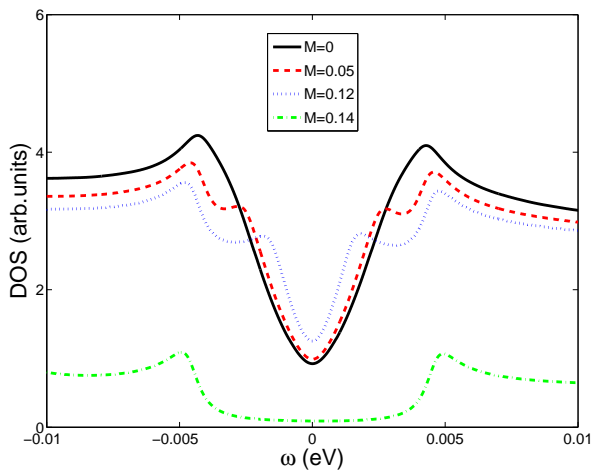


FIG. 1: (color online) The DOS for various SDW gap M . From bottom to top the SDW gap are successively 0.14, 0.12, 0.05, and 0(eV).

These unusual SDW gap dependence of DOS can be understood as follows. After diagonalizing the Hamiltonian (1), we obtain the poles of $G(k, \omega)$, quasiparticle energy bands $\pm E_{\mathbf{k}}^{\pm}$,

$$E_{\mathbf{k}}^{\pm} = \sqrt{(\xi_{\mathbf{k}}^{\pm} - \mu)^2 + \Delta_{\mathbf{k}}^2} \quad (10)$$

with

$$\xi_{\mathbf{k}}^{\pm} = \frac{\varepsilon_{\mathbf{k}} + \varepsilon_{\mathbf{k}+\mathbf{Q}}}{2} \pm \sqrt{\frac{(\varepsilon_{\mathbf{k}} - \varepsilon_{\mathbf{k}+\mathbf{Q}})^2}{4} + M^2} \quad (11)$$

In the normal state, the Fermi surface for the corresponding AF bands ($\xi_{\mathbf{k}}^{\pm} - \mu$) has been plotted in Fig.2, where the dotted-dashed curve is given by the band “+” and the dotted curve by band “-”. At the intermediate value of the SDW gap $M = 0.05$, the FS has been separated into three parts locating around $(\pi, 0)$, $(0, \pi)$ and

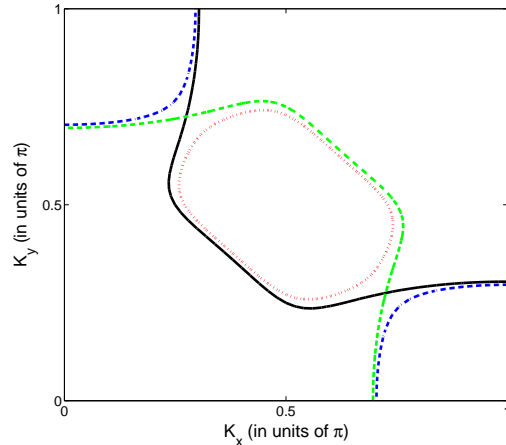


FIG. 2: (color online) Fermi surface for AF bands ($\xi_{\mathbf{k}}^{\pm} - \mu$) with the SDW gap $M = 0.05$. The dotted-dashed curves are contributed by the band “+” and the dotted curve by band “-”. The zero-energy contour of $\varepsilon_{\mathbf{k}}$ (solid curves) and $\varepsilon_{\mathbf{k}+\mathbf{Q}}$ (dashed curves) are shown for reference.

$(\pi/2, \pi/2)$ respectively, which is quite agreement with the ARPES experiment on *NCCO* at the optimal doping²² and the previous theoretical calculations^{10,23}. In this case, the DOS in the SC state obviously shows two different coherent peaks: one at the low energy corresponds to the SC gap maximum opened on the FS piece around $(\pi/2, \pi/2)$, and the other at high energy corresponds to FS pieces around $(\pi, 0)$, and $(0, \pi)$. Therefore the non-monotonic $d_{x^2-y^2}$ -wave behavior gap mentioned above can be satisfactorily explained to the effective gap induced by coexisting AF SDW and SC order. With the decreasing of the SDW, in the limit case $M=0$ (solid curve in Fig.2), the two bands in the FS merge into a single one again, therefore, the DOS shows a V-shaped behavior, similar to that of the hole-doped ones with a monotonic gap^{5,6,23,24}. In contrast, when the SDW increases to be sufficiently large (not shown here), the FS piece around $(\pi/2, \pi/2)$ disappears. As a result, the DOS denoted by dotted-dashed line in Fig.1 behaves to be U-shaped like. As expected above, the SDW gap dependence of FS is qualitatively similar to the intriguing doping evolution of FS²².

In the presence of a single non-magnetic impurity, the LDOS which can be measured in the STM experiment

$$N(r, \omega) = -\frac{1}{\pi} \text{Im} G_{11}(r, r; \omega + i0^{\dagger}) + \frac{1}{\pi} \text{Im} G_{22}(r, r; -\omega - i0^{\dagger}) \quad (12)$$

with the subscripts 11 and 22 refer to the electron and hole part of the diagonal Nambu Green’s function, has been plotted in Fig.3(a)-3(d) for different AF SDW gap, where black solid curve denotes the clean case which is equivalent to DOS, and red dashed curve denotes the

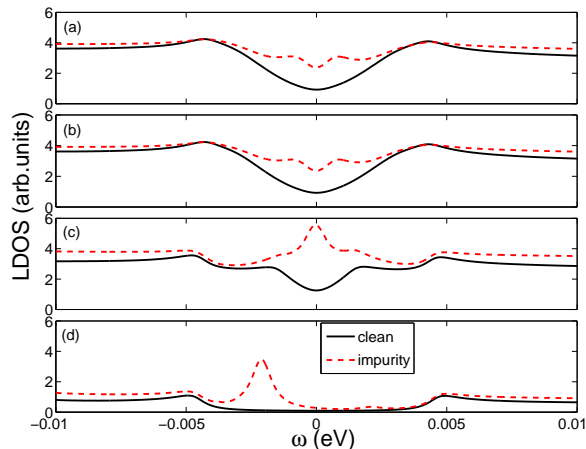


FIG. 3: (color online) The LDOS for various SDW gap M in the clean case and the nearest neighbor of a non-magnetic impurity site. (a) $M = 0$ eV, (b) $M = 0.05$ eV, (c) $M = 0.12$ eV, (d) $M = 0.14$ eV.

nearest neighbor of the impurity site. In the calculation, we take the same parameters as in Fig.1 and set the scattering strength $U_0 = 5$ eV. Note that our results remain qualitatively unchanged when U_0 is varied. Since the DOS remains $d_{x^2-y^2}$ -wave like at low energies for fairly large values M , the two impurity-induced resonance peaks in LDOS appear at positive and negative energy and have different height due to the particle-hole asymmetry, similar to the hole-doped cases¹⁴. As M increases, due to the presence of new “coherence peaks” and an inward shift in the position of them in DOS, two impurity-induced resonance peaks correspondingly shift towards the lower energy and eventually merge into one peak at Fermi energy. For the sufficiently large M , although the DOS behaves to be U-shaped like, two impurity-induced resonance peaks still exist, which is different from the pure s-wave superconductors where no resonance state within the gap was induced by a non-magnetic impurity¹³. Thus we come to a conclusion that U-shaped DOS is due to the coexisting SDW and SC order. We notice that the similar result has also been obtained in the recent paper by Wan *et al* starting with $t - J$ model²⁵.

B. $d_{x^2-y^2}$ -wave with a higher harmonic

In this scenario, we only take the Hamiltonian H_{SC} without AF SDW order term. Based on a scenario in which superconductivity arises from the exchange of AF spin fluctuations, it was argued that the maximum SC gap is achieved near those momenta on the FS (hot spots) that are connected by $Q = (\pi, \pi)^{6,11,26}$. In the electron-doped cuprates, the hot spots are located much closer to the zone diagonal, leading to a non-monotonic behavior

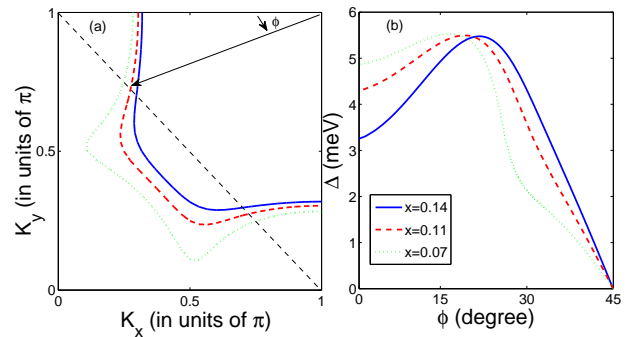


FIG. 4: (color online) (a) The doping (see inset of (b)) dependence of the FS in the one quarter of Brillouin zone. MBZ is denoted by the dashed line and ϕ is the FS angle. (b) corresponding non-monotonic gap as a function of the FS angle ϕ .

of the SC gap. A good fit of $\Delta_{\mathbf{k}}$ to the experimental data is achieved via the inclusion of a higher harmonic, such that $\Delta_{\mathbf{k}} = \Delta_0(\cos(k_x) - \cos(k_y))/2 - \Delta_1(\cos(3k_x) - \cos(3k_y))/2$ with $\Delta_0 = 5.44$ meV and $\Delta_1 = 2.34$ meV ensures that the maximum of $|\Delta_{\mathbf{k}}|$ along the FS is located at the hot spots, as shown by the red dashed curve in Fig.4(a) and Fig.4(b). By tuning the chemical potential and Δ_0 , the doping dependence of FS and correspondingly non-monotonic gap as a function of the FS angle ϕ have also been shown in Fig.4. The other formulas on DOS and LDOS remain.

The doping dependence of LDOS has been plotted in Fig.5, where the black solid curve denotes the clean case which is equivalent to DOS, and red dashed curve denotes the nearest neighbor of the impurity site. It has been shown that for all calculated doping, (i) the DOS at different doping shows two Van Hove singularities at corresponding antinodal gap (Δ_n) and maximum gap at the hot spot (Δ_m), reflecting the presence of a non-monotonic $d_{x^2-y^2}$ -wave gap, (ii) at low energies the DOS spectrum also remains $d_{x^2-y^2}$ -wave like and two impurity-induced resonance states in LDOS locate symmetrically at positive and negative energies and shift towards the low energy with the decreasing doping. These features are similar to that shown in the coexisting AF SDW and SC order scenario for the some small values M (Fig.3(b) and Fig.3(c)). However, we notice that the U-shaped DOS which has been clearly seen in the coexisting SDW and SC phase scenario at large SDW M can not be obtained in the scenario based on $d_{x^2-y^2}$ -wave with a higher harmonic even at underdoped regime (Fig.5(c)). Our results based on the $d_{x^2-y^2}$ -wave with a higher harmonic scenario are quite agreement with the recent doping dependence of tunneling spec-

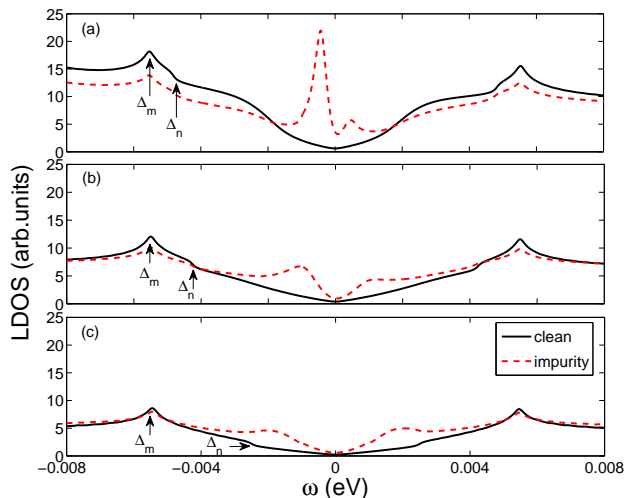


FIG. 5: (color online) The LDOS for various doping in the clean case and the nearest neighbor of a non-magnetic impurity site. (a) $x = 0.14$, (b) $x = 0.11$, and (c) $x = 0.07$. Δ_n and Δ_m denote antinodal gap and maximum gap at the hot spot respectively.

trum measurement⁷, where a non-monotonic gap order parameter for the whole doping range studied has been shown. Therefore, the non-monotonic gap arising from the $d_{x^2-y^2}$ -wave with a higher harmonic due to the peculiar form of the pairing interaction, seems to be more reasonable than the physical origin based on coexisting SDW and SC phase.

IV. CONCLUSION

In summary, motivated by the probably physical origins of the non-monotonic $d_{x^2-y^2}$ -wave gap, we ana-

lyze the DOS and a nonmagnetic impurity effect in the electron-doped cuprates superconductor assuming two different scenarios: the $d_{x^2-y^2}$ -wave superconductivity coexisting with AF SDW order versus $d_{x^2-y^2}$ -wave superconductivity with a higher harmonic originating from the peculiar form of the pairing interaction. We find that in both cases there exist two impurity-induced resonance states at low energies. We also find that for the intermediate value of the SDW gap, the DOS looks similar to that of the $d_{x^2-y^2}$ -wave gap with a higher harmonic. However, if the SDW gap is sufficiently large the DOS looks more conventional s-wave like instead of the non-monotonic $d_{x^2-y^2}$ -wave gap behavior. This obvious difference from that of the $d_{x^2-y^2}$ -wave gap with a higher harmonic even in the underdoped regime, will help to differentiate the two above scenarios and make sure the physical origin of the unusual non-monotonic gap in the electron-doped cuprates. The recent doping dependence of tunneling spectrum measurement⁷ provides the strong evidence of the non-monotonic gap arising from the $d_{x^2-y^2}$ -wave with a higher harmonic, and is qualitatively agreement with our theoretical results. However, the earlier point contact tunneling spectrum and penetration depth measurement show the U-shaped DOS, suggesting the coexisting SDW and SC order. Therefore, in order to reach the consensus on this topic, our results strongly suggest the further doping dependence of tunneling spectrum measurement, especially in the underdoped regime, is needed to be carried out as soon as possible.

Acknowledgments

We thank Ilya Eremin and Jun Chang for many useful discussions. Y.L. acknowledges support from National Natural Science Foundation of China under Grand Nos.10404001.

¹ See e.g., A.J. Millis, A. Zimmers, R.P.S.M. Lobo, N. Bonetemp, and C.C. Homes, Phys. Rev. B **72**, 224517 (2005).
² C.C. Tsuei, and J.R. Kirtley, Phys. Rev. Lett. **85**, 182 (2000).
³ Guo-qing Zheng, T. Sato, Y. Kitaoka, M. Fujita, and K. Yamada, Phys. Rev. Lett. **90**, 197005 (2003).
⁴ H. Matsui, K. Terashima, T. Sato, T. Takahashi, M. Fujita, and K. Yamada, Phys. Rev. Lett. **95**, 017003 (2005).
⁵ N.P. Armitage, D.H. Lu, D.L. Feng, C. Kim, A. Damascelli, K. M. Shen, F. Ronning, Z.-X. Shen, Y. Onose, Y. Taguchi, and Y. Tokura, Phys. Rev. Lett. **86**, 1126 (2001).
⁶ G. Blumberg, A. Koitzsch, A. Gozar, B.S. Dennis, C.A. Kendziora, P. Fournier, and R.L. Greene, Phys. Rev. Lett. **88**, 107002 (2002).
⁷ Y. Dagan, R. Beck, and R.L. Greene, Phys. Rev. Lett. **99**, 1407004 (2007).
⁸ C.C. Homes, R.P.S.M. Lobo, P. Fournier, A. Zimmers, and

R.L. Greene, Phys. Rev. B **74**, 214515 (2006).
⁹ H. Yoshimura and D.S. Hirashima, J. Phys. Soc. Jpn. **73**, 2057 (2004); J. Phys. Soc. Jpn. **74**, 712 (2005).
¹⁰ Q.S. Yuan, Y. Chen, T.K. Lee, and C.S. Ting, Phys. Rev. B **69**, 214523 (2004); Q.S. Yuan, F. Yuan, and C.S. Ting, Phys. Rev. B **73**, 054501 (2006).
¹¹ D. Manske, I. Eremin, K.-H. Bennemann, Phys. Rev. B **62**, 13922 (2000).
¹² Bin Liu, and I. Eremin, unpublished.
¹³ L. Yu, Acta. Phys. Sin **21**, 75 (1965); H. Shiba, Prog. Theor. Phys **40**, 435 (1968); A.I. Rusinov, Sov. Phys. JETP **29**, 1101 (1969).
¹⁴ Q.H. Wang and Z.D. Wang, Phys. Rev. B **69**, 092502 (2004); Dirk.K. Morr, Phys. Rev. Lett. **89**, 106401 (2002)
¹⁵ Tanmoy Das, R.S. Markiewicz, and A. Bansil, Phys. Rev. B. **74**, 020506R (2006).
¹⁶ Ø. Fischer, M. Kugler, I. Maggio-Aprile, C. Berthod, and

- C. Renenr, *Rev. Mod. Phys.* **79**, 353 (2007); A.V. Balatsky, I. Vekhter, and Jian-Xin Zhu, *Rev. Mod. Phys.* **78**, 373 (2006).
- ¹⁷ Q.H. Wang, *Phys. Rev. Lett.* **88**, 057002 (2002).
- ¹⁸ C. Kusko, R.S. Markiewicz, M. Lindroos, and A. Bansil, *Phys. Rev. B.* **66**, 140513R (2002).
- ¹⁹ H.J. Kang, P.C. Dai, J.W. Lynn, M. Matsuura, J.R. Thompson, S.C. Zhang, D.N. Argyriouk, Y. Onose, and Y. Tokura, *Nature* **423**, 522 (2003); H.J. Kang, P.C. Dai, H.A. Mook, D.N. Argyriouk, V. Sikolenko, J.W. Lynn, Y. Kurita, S. Komiya, and Y. Ando, *Phys. Rev. B* **71**, 214512 (2005).
- ²⁰ L. Alff, S. Meyer, S. Kleefisch, U. Schoop, A. Marx, H. Sato, M. Naito, and R. Gross, *Phys. Rev. Lett.* **83**, 2644 (1999); S. Kashiwaya, T. Ito, K. Oka, S. Ueno, H. Takashima, M. Koyanagi, Y. Tanaka, and K. Kajimura, *Phys. Rev. B* **57**, 8680 (1998).
- ²¹ A. Biswas, P. Fournier, M.M. Qazilbash, V.N. Smolyaninova, H. Balci, and R.L. Greene, *Phys. Rev. Lett.* **88**, 207004 (2002); J.A. Skinta, M.-S. Kim, T.R. Lemberger, T. Greibe, and M. Naito, *ibid.* **88**, 207005 (2002).
- ²² N.P. Armitage, F. Ronning, D.H. Lu, C. Kim, A. Damascelli, K. M. Shen, D.L. Feng, H. Eisaki, Z.-X. Shen, P.K. Mang, N. Kaneko, M. Greven, Y. Onose, Y. Taguchi, and Y. Tokura, *Phys. Rev. Lett.* **88**, 257001 (2002).
- ²³ C.S. Liu, H.G. Luo, W.C. Wu, and T. Xiang, *Phys. Rev. B* **73**, 174517 (2006).
- ²⁴ A. Snezhko, R. Prozorov, D.D. Lawrie, R.W. Giannetta, J. Gauthier, J. Renaud, and P. Fournier, *Phys. Rev. Lett.* **92**, 157005 (2005).
- ²⁵ Y. Wan, H.D. Lü, H.Y. Lu, and Q.H. Wang, *Phys. Rev. B* **77**, 064515 (2008).
- ²⁶ P. Krotkov, and A.V. Chubukov, *Phys. Rev. Lett.* **96**, 107002 (2006); *ibid.* *Phys. Rev. B* **74**, 014509 (2006).